Modelling liver cancer microenvironment: novel 3D culture system as a potential anti-cancer drug screening tool

Ala'a Al Hrout[1,2], Karla Cervantes-Gracia[1], Richard Chahwan[1]*, Amr Amin[2,3]*

[1] Institute of Experimental Immunology, University of Zurich, 8057 Zurich, Switzerland

[2] Biology Department, College of Science, UAE University, P.O. Box 15551, Al-Ain, UAE

[3] The University of Chicago, Chicago, IL 60637, USA

*** Equal contributing authors and to whom correspondence should be addressed:**

Prof Amr Amin
Biology Department, UAE University, Al Ain P.O.Box: 15551, UAE.
Tel: +971 3 7136519
Fax: +971 3 6761291
Email: a.amin@uaeu.ac.ae
Or
Prof Dr Richard Chahwan
Institute of Experimental Immunology, University of Zurich, Winterthurerstrasse 190, Y23K74, Zurich 8057, Switzerland
Tel: +41 446353710
Fax: +41 446356883
Email: chahwan@immunology.uzh.ch

Running title: 3D multicellular organoid system mimics the tumor milieu

Keywords: 3D co-culture, transcriptomic, proteomics, systems biology, ex vivo cancer modelling.

Word count: ~5,349

ABSTRACT

The tumor microenvironment and its contribution to tumorigenesis has been a focal highlight in recent years. A two-way communication between the tumor and the surrounding microenvironment sustains and contributes to the growth and metastasis of tumors. Progression and metastasis of hepatocellular carcinoma have been reported to be exceedingly influenced by diverse microenvironmental cues. In this study, we present a 3D-culture model of liver cancer to better mimic *in vivo* tumor settings. By creating novel 3D co-culture model that combines free-floating and scaffold based 3D-culture techniques of liver cancer cells and fibroblasts, we aimed to establish a simple albeit reproducible *ex vivo* cancer microenvironment model that captures tumor-stroma interactions. The model presented herein exhibited unique gene expression and protein expression profiles when compared to 2D and 3D mono-cultures of liver cancer cells. Our results showed that in vivo like conditions cannot be mimicked by simply growing cancer cells as spheroids, but by co-culturing them with 3D fibroblast with which they were able to cross-talk. This was evident by the upregulation of several pathways involved in HCC, and the increase in secreted factors by co-cultured cancer cells, many of which are also involved in tumor-stroma interactions. Compared to the conventional 2D culture, the proposed model exhibits an increase in the expression of genes associated with development, progression, and poor prognosis of HCC. Our results correlated with an aggressive outcome that better mirrors *in vivo* HCC, and therefore, a more reliable platform for molecular understanding of HCC and possibly better anti-cancer drug screening.

INTRODUCTION

Cancer is a multi-factorial disease, arising from normal cells, primarily through abnormal cellular proliferation and progressive mutation load. Tumor cells, however, represent only one aspect of tumorigenesis. The tumor milieu is composed of a dynamic network of non-malignant cellular components, non-cellular components, signaling molecules, and extracellular matrix (ECM) [1,2], which collectively forms the tumor microenvironment (TME). A dynamic two-way communication between the tumor and the surrounding milieu, sustains and contributes to tumor growth and metastasis [3]; thereby highlighting the key role the TME plays in tumor progression [1,4]. In addition, many studies have reported the positive role of the TME in restraining tumor initiation and progression at initial stages of carcinogenesis [5], and how "re-programming" the TME in the later stages holds a great potential for developing effective cancer treatments [1].

Fibroblasts are generally considered the predominant cellular TME component. Whilst normally in an "inactive" quiescent state; fibroblasts recruited to the tumor site are constantly activated by the tumor through paracrine signaling, after which they are transformed into cancer-associated fibroblasts (CAFs) [6]. Once the CAF transition is triggered, paracrine signaling is no longer needed [7]. These transformed CAFs become distinct in their morphology and function from normal fibroblasts [7], most likely due to their rewiring by tumor signaling. CAFs possess higher ability to proliferate [8], be tumor proximal, and evade apoptosis [9]. But the molecular mechanisms mediating this process remains elusive. CAFs contribute significantly to tumorigenesis; partly through suppressing immune responses, secreting growth factors, cytokines, and proangiogenic factors [10]. In addition, CAFs contribute to tumorigenesis through secreting ECM proteins and degrading matrix metalloproteinase (MMPs), which together, give CAFs their ECM remodeling ability [10]. CAFs, therefore, have potential as therapeutic targets [11].

A tumor has an increasing demand for oxygen and nutrients to support its progression. When the demand for oxygen remains unmet, low oxygen hypoxic conditions ensue [12]. To survive, tumor cells activate the hypoxia-inducible factor 1 (HIF1) [12], which in turn activates the transcription of a group of genes through binding to their hypoxia-response elements to

promote the survival of tumor cells [13]. HIF-1 targeted genes significantly contribute to tumor angiogenesis, metastasis, adhesion, metabolism, and pH regulation [13]. Moreover, many studies have highlighted the role of hypoxia in recruiting stromal components to the TME [14], ECM composition, and metastatic remodeling [15]

Hepatocellular carcinoma (HCC), is the fifth most common cancer and is the fourth cause of cancer-related death worldwide [16]. HCC has a very poor prognosis with only five-year survival rate [17]. HCC progression is influenced by the liver microenvironment such as altered stromal cells [18]. These cells deposit ECM proteins causing fibrosis that then progresses to cirrhosis with a prevalence of 80-90% [18]; suggesting a crucial role of ECM build-up in HCC progression [19]. Hypoxia represents a driving force for HCC progression, and is associated with poor prognosis [20]. HIF-mediated gene expression contributes to different aspects of HCC metastasis, such as epithelial mesenchymal transition (EMT) [21], invasion of the ECM, and metastasis [22]. Yet the molecular mechanisms governing stromal and tumor cell interactions within the TME of HCC under hypoxic conditions [14] remains unclear.

To reflect the complexity and dynamic nature of tumor cell biology, a physiologically relevant model is needed. Especially, when it comes to drug discovery and identifying effective therapeutic targets. To simulate *in vivo* environment, *in vitro* two-dimensional (2D) cell culture is typically assembled by growing cells *commonly* on a plastic substrate in an adherent monolayer. However, distortion of spatial arrangement of cells in 2D culture changes cell-cell and cell-matrix interactions [23], and most importantly, alters the response of cells to certain drugs and treatments [24]. That is why, 3D cultured cells better recapitulates *in vivo* architecture of tumors and exhibits gene expression closer to that of *in vivo* tumors [23]. One very common 3D cultured cells model is the spheroid; a micro cell cluster sphere [25]. The nature of this three-dimensional multicellular model is what makes it an attractive tool to simulate solid tumors *in vitro* as it is composed of three regions, a highly proliferative outer region, a middle quiescent region, and a hypoxic core region [26]. Such compartmentalization creates diffusional gradients of oxygen, nutrients, and tested drugs among all three regions of the spheroid, which is also characteristic of solid tumors [27].

We aimed at modeling the basic TME of liver cancer by mimicking certain aspects of in vivo tumors, such as three-dimensionality of tissue, hypoxia, and heterogeneity of tumors. Five groups were designed to reflect each element, group 1 is a control group for comparison purposes which consists of 2D mono-cultures of liver cancer cells. Group 2 is also 2D mono-cultures of liver cancer cells but induced for hypoxia chemically. Group 3 on the other hand is like group 2 but additionally includes conditioned media from 2D fibroblasts to reflect a one-way co-culture system. Group 4 and 5 are 3D cultures of liver cancer cells that exhibit hypoxia physiologically due to culturing conditions. However, group 5, which is our proposed model, includes a 3D culture of fibroblast in a separate insert, reflecting a two-way co-culture system. Our findings reported herein demonstrate that our proposed model of group 5 reflects many aspects of in vivo settings and signaling pathways, promoting it as a potential platform for further studies of drug efficacy in vitro and understanding the communication between cancer and the stroma in liver cancer.

MATERIALS AND METHODS

Co-culture Systems

For the 2D co-culture, a one-way communication system was followed. Briefly, HepG2 and SV-80 cells were seeded at a density of 1X 10^6 in conventional 2D culturing flasks in DMEM media. Flasks were incubated at 37°C in 5% CO_2 humidified incubator for about 24 hours. Conditioned media of SV-80 cell line was collected, centrifuged to collect any cellular debris, and applied to HepG2 cells, which were incubated with the conditioned media for 48 hours.

For the 3D co-culture, a two-way communication system was followed. Briefly, HepG2 and SV-80 3D cultures were prepared separately. Prior to co-culture, 6-well plates were coated with 1.5% agarose, and allowed to set and cool before transferring HepG2 spheres to the bottom of the coated plates, and the inserts containing SV-80 3D culture were placed on top. HepG2 and SV-80 3D cultures were incubated for 48 hours.

The remaining materials and methods are included in supplementary data.

RESULTS

Comparing 2D, mono- 3D, and co- 3D cultures and their gene expression

Fibroblasts grown as a 2D culture exhibit an elongated morphology. However, growing fibroblasts as 3D culture in porous scaffolds alters their morphology to be more rounded. HepG2 cells grown in 3D were monitored over a period of 5 days to assess formation of tight spheroids with a smooth surface (Fig. 1A-B. HepG2 2D cultures were treated with increasing concentrations of $CoCl_2$ (100-400 µM) to assess cellular viability under hypoxia-mimicking conditions (Fig. 1C). Treatment of HepG2 with $CoCl_2$ did not affect cellular viability significantly at doses of 100 and 200 µM of $CoCl_2$. However, a highly significant difference ($p < 0.001$) was noted at a dose of 400 µM $CoCl_2$. To confirm the induction of hypoxia in $CoCl_2$- treated HepG2 2D cultures, protein expression of HIF1α was assessed using western blot. Treatment with 200 µM of $CoCl_2$ for 6 hours did not induce HIF1α expression. However, by increasing the dose to 300 µM, HIF1α expression was detected in HepG2 cells (Fig. 1D). Immunofluorescence was then used to detect the cellular localization of HIF1α, showing that $CoCl_2$ also affects HIF1α translocation to the nucleus (Fig. 1E), where it can bind to hypoxia-response elements (HREs).

Differential gene expression analysis

To better assess in vivo mimicking capabilities of our 5 groups, RNA from the denoted samples (Fig. 1A) were extracted and then sequenced via the Illumina platform. Significant differentially expressed genes (DEGs) were determined at a cutoff of Log2FC of 1 and FDR < 0.05. A hierarchical clustering Heatmap was used to explore changes in global gene expression across our 5 models (Fig. 2 A). Interestingly, group 5 clustered separately from the rest, revealing a fundamental and distinctive change in gene expression. Principal component analysis (PCA) based on the global gene expression showed a similar outcome, where group 5 segregated at the opposite extreme of all other groups, with the conventional HepG2 culture (group 1) being the most distant (Fig. 2B), suggesting fundamental differences between 2D, monocellular 3D, and multicellular 3D models.

Significant differentially expressed genes (DEG) were determined relative to group 1 using RNA-seq 2G. Group2 resulted in significant upregulation of 243 genes and downregulation of 131

genes. Group3 increased the number of significantly DEGs to 474 upregulated and 145 downregulated genes. When comparing gene expression profile of group 4 to group 1, 203 genes were significantly upregulated, whereas 82 genes were downregulated. Group 5 dramatically changed the gene expression of HepG2 by significantly upregulating 1291 and downregulating 880 genes in group 5 in comparison to group 1. PCA plot based on the DEGs showed similar results to the global expression PCA plot, whereby group 5 was segregating separately from the remaining groups (Fig. 2C). In Addition, significant DEGs signatures, unique to each group, were identified (Fig. 2D). Group 5 exhibited the highest number in unique significant DEGs among all other groups, at 957 upregulated genes and 796 downregulated genes. A full List of common and unique significantly DEGs of each group is available in supplementary files 1 and 2.

Canonical pathways associated with significant DEGs in different culturing conditions were analyzed using gene-based enrichment analysis by XGR. As expected, culturing HepG2 cells under hypoxia-mimicking conditions (group 2 and 3) upregulated genes involved in hypoxia-inducible factor-1 alpha (HIF1-α) and hypoxia-inducible factor-2 alpha (HIF2-α) pathways, and networks downstream of these pathways. This was even observed in 3D spheroid cultures (group 4 and 5) despite not being treated with a hypoxia inducing agent, indicating the formation of hypoxic core in 3D culture spheroids. Culturing HepG2 cells with only fibroblasts conditioned media (group 3) or alternatively with 3D culture of fibroblasts (group 5) upregulated genes involved in integrin family cell surface interactions, interleukin-6 (IL6) mediated signaling events (Table S1).

In-depth pathway functional analysis reveals pathways associated with HCC progression.

To further understand the role of significant DEGs in each group, we applied clustering analysis using ClueGO/CluePedia as described previously [28] . By combining Gene Ontology (GO) terms, KEGG and Wiki pathways, ClueGo/CluePedia create a better interpretation of the pathways associated with the list of input genes [29] . Hypoxia mimicking conditions in group 2 induced cellular responses to hypoxia and HIF-1 signaling pathway, as well as other signaling pathways reported to promote HCC including NRF2, FOXO, and p53 pathways [30,31] (Fig. 3A-B).

Similarly, inducing hypoxia in group 3 resulted in inducing HIF-1 signaling pathways. However, with the addition of fibroblast conditioned media, group 3 DEGs-associated processes were enriched in 3 out of 5 pathways previously reported in KEGG analysis of HCC patients' tissues including i) complement and coagulation cascades, ii) focal adhesion, and iii) ECM-receptor interaction [32] (Fig. 3A). DEGs-associated processes of HepG2 3D culture alone (group 4) resembled some of group 2 such as hypoxia and NRF2 signaling pathways, but also some of group 3 such as G3 such as complement and coagulation cascades (Fig. 3A). Additionally, DEGs-associated processes of group 4 included steroid hormone biosynthesis process and estrogen signaling pathway, which have been linked to HCC progression [33] (Fig. 3A). Group 5 shared some pathways with the other groups such as hypoxia, focal adhesion, glycolysis/ gluconeogenesis, and estrogen signaling pathway. In addition, DEGs-associated processes of group 5 were significantly enriched in HCC-promoting pathways including oncostatin M signaling pathway, insulin signaling pathway and aryl hydrocarbon receptor pathways [34,35] (Fig. 3B).

After identifying the main pathways involved in group 5 through ClueGO/CluePedia clustering, Insulin signaling pathway was further analyzed and visualized in PathVisio due to its documented relevance in HCC [36] and to gain insights of significant physiological changes occurring within a specific pathway. Genes below FDR 0.05 (5871 hits) were imported into PathVisio [37] to identify trends in regulation within this particular pathway and other chained events embedded within associated pathways. Inconsistencies within these maps were excluded from the final pathway (Fig. 4). The Insulin signaling pathway in group 5 was found to mainly lead to activation of genes involved MAPK signaling and this trend converges with hypoxia signaling input, both leading to the production of VEGFB, VEGFA, PGF, growth factors known to be involved in angiogenesis and tumor invasion [38]. Tumor invasion can also be promoted via Ras and its downstream pathways of MAPK and RALB, which were all shown to be upregulated in group 5. Some of the genes involved in the pathway shown previously have been validated with qPCR (Fig. 5A).

Co-culture of Fibroblasts and HepG2 3D cultures enriches the secretome in pro-tumor factors

To identify signaling factors playing a role in the crosstalk between cancer cells and fibroblasts, the secretome of group 4 and 5 was analyzed for factors involved in angiogenesis, invasion, and metastasis, in addition to other factors in the insulin signaling pathway, secretome of 3D fibroblasts was included as a control (Fig S2, Fig. 5B-F). Most factors were dramatically increased in the secretome of group 5 (from both fibroblasts and HepG2 cells) when compared to 3D mono-cultures. Co-culturing HepG2 spheroids with 3D culture of fibroblasts increased the levels of insulin signaling pathway factors like IGF-II, IGFBP1, IGFBP2 (Fig 5B). In addition, levels of different angiogenesis and cytokines that are involved in the cross-talk in the TME were highly increased in the setting of group 5 (Fig 5C & F).

As the secretome collected from group 5 is shared among fibroblasts and HepG2 cells, we wanted to confirm the source of the secreted factors. To that end we compared gene expression of 3D HepG2 or 3D fibroblasts before and after co-culture (group 5 over group 4) (Fig. 5G). Differential gene expression analysis revealed that M-CSF, IGFBP1, IGFBP2, TGF-β, and PECAM-1 were upregulated in HepG2 cells after co-culture, while they were not differentially expressed in fibroblasts. On the other hand, TGF-α, and IL-1β were only differentially expressed in fibroblasts after co-culture. VEGF and IGF-II were differentially expressed in both HepG2 cells and fibroblasts, being more upregulated in HepG2 cells (Fig. 5G). Despite that VEGF is upregulated more than 2.5 folds on the RNA level in HepG2 cells after co-culture (Fig. 5G), there was no noticeable difference in the secreted VEGF from 3D HepG2 cells before and after co-culture (Fig. 5F). Nonetheless, VEGFR2 was more expressed in group 5 in comparison to group 1 and group 4; while VEGFR1 was higher in the 3D cultures, but no noticeable difference between the two (Fig. 5H). TNFR1 was also dramatically higher in group 5 when compared to both group 1 and group 4 (Fig. 5H). Kaplan-Meier curves of genes within our main pathway of interest were analyzed. IGF1R and EGLN3 showed a significant correlation between expression and prognosis (Fig. 5 I-J). Both genes were shown to be involved in insulin signaling pathway (Fig. 4).

Pathway complementation analysis highlights regulatory miRNAs and prognosis markers

To better understand the changes elicited by the 3D co-culture conditions on HepG2 cells, we investigated the effect of miRNA regulation given their role in affecting *de novo* or modulating

established gene expression in tumors [39,40]. Based on miRNA-gene interaction analysis of significant DEGs in group 5, miR-335 was the top regulatory miRNA with the highest number of connections to other genes in the network (Fig. S4 A). Other miRNAs were predicted, top 10 are shown in Fig. S4 B with literature citations (full list is available in Table S2).

DISCUSSION

Establishment of 3D culture models

We investigated the bilateral effect of the cellular architecture and milieu on the properties and phenotypic responses of the whole cellular microenvironment of tumor cells. Liver cancer microenvironment was modeled using 2D and 3D mono- and co-culture systems. The transcriptome of five models was profiled to determine the effects of each condition. Each one of the culturing conditions mimicked an aspect of the TME. Based on our clustering methods, group 5 clustered away all the other groups, specifically group 1, in both the PCA plot and hierarchical cluster heatmap (Fig. 2 A-C). This is in line with the Venn diagram, where group 5 had the highest number of unique genes that are not shared with other groups (Fig. 2D). This clear distinction suggests a fundamental difference in gene expression between the proposed model of group 5 and all other culturing conditions, signifying a considerable change in gene expression as a result of 3D co-culture of cancer spheroids with fibroblasts.

Mimicking hypoxic conditions is not sufficient to mimic *in vivo* conditions

Treatment with hypoxia mimicking agent significantly upregulated genes associated with p53 and AP-1 networks (Table S1). AP-1 proteins (*i.e.* Jun, Fos, and ATF families) are activated by hypoxia and are frequently deregulated in cancer [41]. Deregulation of ATF-2 and its network have been implicated in liver development, regeneration, and cirrhosis [42]. In addition, ATF-2 has been reported to play a role in HCC resistance to sorafenib, *in vivo* [43]. The presented hypoxia mimicking conditions also induced several metabolism pathways including fructose, mannose, starch, and sucrose metabolism; as well as glycolysis and gluconeogenesis (Fig. 3). Nonetheless, without treatment with $CoCl_2$, HepG2 spheroids (group 4 & 5) upregulated genes were associated with HIF1-α and HIF2-α (Fig. 3A; Table S1). This is consistent with studies promoting cancer spheroids as candidate solid tumor model, as they recapitulate many aspects

of *in vivo* tumors including hypoxia [44]. Hypoxia-mediated pathways in turn promote survival, angiogenesis, invasion, and metastasis [45]. Hypoxia also plays a role in lipid and steroid metabolism [46]. Steroids promote tumor immune evasion by suppressing T cell activation and subsequently effecting immune-therapy outcome [47]. This is consistent with induction of steroid synthesis and estrogen signaling pathways in group 4 and 5 (physiological hypoxia), but not group 2 and 3, suggesting that chemically mimicking hypoxia is not sufficient to recapitulate a more encompassing hypoxic condition (Fig. 3; Table S1). Taken together, these results demonstrate how adjusting HepG2 cells from 2D to 3D culture introduces hypoxia and its associated hallmarks, which better represents *in vivo* cancer conditions.

Reconstitution of the dynamic bilateral interaction between cancer and stromal cells through 3D co-culture system

Studying the interaction between cancer cells, stromal fibroblasts, and their contribution to tumorigenesis remains a challenge. We, therefore, created a simplified system to mimic stroma-tumor interaction. HepG2 cells were either cultured with fibroblasts conditioned media only (group 3) to mimic one-way interaction or cultured with fibroblasts in a 3D-culture system (group 5) to mimic a two-way communication. When cultured with fibroblasts, HepG2 upregulated genes were associated with integrin cell surface interactions, in addition to urokinase-type plasminogen activator (uPA) and uPAR-mediated signaling. Integrin signaling pathway (ISP) regulates the interaction with the extracellular environment in response to intracellular cues [48] β1 integrins are overexpressed in many tumors, and blocking their signaling transduction reduces survival and tumorgenicity of many cancers, in 2D and 3D *in vitro* cultures, and *in vivo* [49–52]. ISP transduction has been reported to be promoted by other cell surface proteins, such as urokinase receptor (uPAR) [53]. Suppressing uPAR expression or disruption uPA/uPAR interaction have been reported to inhibit tumor progression and metastasis [54]. In addition, canonical pathways associated with the upregulated genes in group 3 and 5 included IL-6 mediated signaling. This is consistent with Integrin increased signaling, where enhanced IL-6/STAT3 signaling is promoted by β1-Integrin pathway [55,56]. IL-6 overexpression has been reported in many cancers, including HCC, where it is suggested to

promote the transition of fibroblasts to CAFs [57]. Indeed, studies have shown CAFs as the main source of IL-6, promoting survival, migration, invasion, angiogenesis and stemness in colorectal, gastric, and liver cancer cells [58]. By co-culturing HepG2 cells with fibroblasts, we were able to recapitulate signaling pathways essential in tumor-stroma crosstalk, creating a more reliable model to study complex TME interactions.

Recapitulating signaling pathways in HCC through 3D co-culture system

Insulin/IGF signaling pathway is known to be activated in many cancers including HCC. Studies have shown its essential role in carcinogenesis and metastasis [59]. The insulin pathway was generally activated in 3D model (group 5) in comparison to other culturing methods. Many of the factors involved in insulin pathway – in addition to factors involved in hypoxia, angiogenesis, and MAPK signaling – were upregulated in our study (Fig. 3 & 4); which was confirmed on the transcriptome and secretome levels (Fig. 5). HK1 is dramatically upregulated in group 5 (Fig. 5a). HK1 shows involvement in glycolysis, HIF, and insulin signaling pathways (Fig. 3A-B), a role that has been reported in various studies; where HK1 contributes to glycolysis, proliferation, migration, and invasion of HCC [40,60,61]. Similarly, PFKFB3, a direct target of HIF1, is upregulated in all groups in comparison to group 1 and regulates glucose metabolism and promotes cancer progression and growth [62]. Overexpression of PFKFB3 is associated with poor prognosis of HCC, and its inhibition resulted in suppression of HCC growth *in vitro* and *in vivo* [63] and reversed the in vitro sorafenib-resistance of HCC cells [64]. EGLN3, that mediates crosstalk between hypoxia and insulin signaling pathways [65,66], was upregulated in HCC hypoxic settings [67,68]. Consistently, EGLN3 was a significant factor driving hypoxia and insulin pathways in our proposed model (group 5). Culturing HepG2 under 3D co-culture conditions also enhanced the expression of genes promoting angiogenesis, migration, and invasion such as SERPINE1, ETS1, MMP3, and MMP7. ETS1, MMP3, and MMP7 are only upregulated in group 5 in comparison to group 1. ETS1 is involved in upregulating hypoxia-target genes such as MMP3, and MMP7 [69,70]. Downregulation of ETS1 was reported to inhibit metastasis and invasion of liver cancer cell lines [71]. Similarly, Expression of MMP3 and MMP7 is correlated with enhanced metastatic phenotype, where their inhibition suppressed

invasion and migration of HCC cells [18]. SERPINE1 was distinctively upregulated in all groups compared to group 1, yet, with the highest fold change exhibited in group 5. Increased expression of PAI-1 (encoded by SERPINE1) is correlated with aggressive cancers and poor prognosis, where it is also associated with migration, invasion, and angiogenesis in HCC tissue [72]. Culturing HepG2 under 3D co-culture conditions also downregulated the expression of genes involved in cell cycle regulation and survival, including E2F2, E2F7, and E2F8. E2F transcription factors were only differentially expressed in group 5, where they were found to be downregulated in comparison to group 1, as confirmed by qPCR (Fig. 5a). Downregulation of E2F2, E2F7, and E2F8 prevents cell cycle arrest and enhances clonogenic survival [73]. Taken together, these findings indicate that culturing HepG2 in a 3D co-culture system (group 5) results in enhanced migration, invasion, metastasis, and angiogenesis, and successfully recapitulating many signaling pathways that are important in HCC *in vivo*.

Pathway complementation analysis highlights the involvement of regulatory miRNAs

The cross-talk between cancer cells and other cells in the TME is also partly mediated through expression of miRNA and/or release of miRNAs through extracellular vesicles (EVs) [74]. Gene-miRNA interaction network analysis of significant DEGs of group 5 revealed a number of predicted regulatory miRNAs (Fig. S4, full list in Table S2), many of which are signature of HCC deregulated miRNAs [39,60]. For instance, miR-335 had the highest number of connections in group 5 (Fig. S4 a). Serum of HCC patients undergoing TACE was analyzed for circulating miRNAs level, where miR-335 level was associated with significantly poor prognosis [75]. Thus, EV miR-335 has been suggested as a novel therapeutic strategy as it was shown to be involved in proliferation and invasion both in vitro and in animal model [76]. Our data suggest an interesting role of EV-based communication that could be explored in the future using our novel 3D co-culture HCC model, which resembles a simplified setting of the TME.

Secretome profiling in our 3D co-culture supports genes expression profiling and recapitulates *in vivo* signatures

Cellular communication between cancer cells and their surrounding is partially driven by secreted proteins and other soluble factors including cytokines, chemokines, and growth factors. Using antibody microarrays, we determined the levels of different factors and their binding proteins that play a role in insulin pathway, angiogenesis, and cytokine signaling (Fig. 5 B-F). Our results show that secretion of insulin/ IGF pathway proteins IGF-2, IGFBP1, and IGFBP2 is increased by co-culturing HepG2 cells with fibroblasts under 3D co-culture conditions in comparison to mono-cultures (Fig. 5 B & G). IGF-2 is upregulated in several tumors including HCC. Its overexpression was notably detected in HCC patient and was shown to induce liver tumor formation, proliferation and angiogenesis in mice [36]. IGF binding proteins (IGFBPs) are essential in the IGF signaling axis, where they bind with high affinity to IGF-1 and IGF-2, and have been reported in HCC patients [59,77]. Granulocyte-, macrophage-, and granulocyte-macrophage- colony-stimulating factors (G-, M-, GM-, respectively) secreted levels have all increased in 3D co-culture setting in comparison to mono-cultures (Fig. 5 E & G). G-CSF, M-CSF, and GM-CSF have been shown to be involved in liver regeneration, fibrosis, angiogenesis, and initiation and progression of liver cancer [78]. Similarly, levels of factors involved in angiogenic pathway including growth factors, angiopoietins, and matrix metalloproteinases are increased by co-culturing HepG2 cells with fibroblasts under 3D culture conditions (Fig. 5 C & F-H). Despite that the 3D model we are proposing herein is restricted to cancer cells and fibroblasts, present data interestingly shows that our 3D model (group 5 settings) increase the secretion of several cytokines known to orchestrate the cross-talk between the tumor and its immune TME (Fig. 5 D & G-), triggering pro-tumor inflammation and immunosuppression [79]. Our pathway complementation analysis also highlighted two of the enriched genes of group 5 as prognostic markers, namely IGF1R an EGLN3 (Fig. 5 I-J). Both have been reported as indicators of poor HCC prognosis [68,80,81].

In conclusion, we propose a novel 3D tissue culture model of liver cancer that better mimics *in vivo* settings. Compared to the conventional 2D culture, the proposed model exhibits an increase in the expression of genes associated with development, progression, and poor prognosis of HCC. Our results showed that in vivo like conditions cannot be mimicked by simply

396 growing cancer cells as spheroids, but by co-culturing them with 3D fibroblast with which they
397 were able to cross-talk. This was evident by the upregulation of several pathways involved in
398 HCC, and the dramatic jump in secreted factors and surface receptors by co-cultured cancer
399 cells, many of which are also involved in tumor-stroma interactions. We have explored the
400 aspects of HCC our proposed model mimic by combining transcriptome and small scale-
401 secretome analysis, which could be expanded in the future to include proteome analysis.
402 Compared to the conventional 2D culture, the proposed model exhibits an increase in the
403 expression of genes associated with development, progression, and poor prognosis of HCC. Our
404 results correlated with a robust phenotype that better mirrors *in vivo* HCC, from gene
405 expression to prognosis markers, and therefore, a more reliable platform for molecular
406 understanding of HCC and possibly better anti-cancer drug screening platform.
407
408
409

410 **Acknowledgements**

411 KCG is supported by a CONACYT scholarship (2019-000021-01EXTF-00542). RC is supported by SNF
412 (CRSK-3_190550), BBSRC (BB/N017773/2), and the UZH Research Priority Program (URPP) "Translational
413 Cancer Research". AA is supported by ZCHS (31R174), UPAR (31S319), and Terry Fox Foundation
414 (21S103).
415
416
417

418 **Competing financial interests**

419 The authors declare no competing interests.

References

[1] Quail DF, Joyce JA. Microenvironmental regulation of tumor progression and metastasis. Nat Med 2013;19:1423–37. https://doi.org/10.1038/nm.3394.

[2] Catalano V, Turdo A, Di Franco S, Dieli F, Todaro M, Stassi G. Tumor and its microenvironment: A synergistic interplay. Semin Cancer Biol 2013;23:522–32. https://doi.org/10.1016/j.semcancer.2013.08.007.

[3] Hanahan D, Weinberg RA. Hallmarks of cancer: The next generation. Cell 2011;144:646–74. https://doi.org/10.1016/j.cell.2011.02.013.

[4] Hanahan D, Coussens LM. Accessories to the Crime: Functions of Cells Recruited to the Tumor Microenvironment. Cancer Cell 2012;21:309–22. https://doi.org/10.1016/j.ccr.2012.02.022.

[5] Bissell MJ, Hines WC. Why don't we get more cancer? A proposed role of the microenvironment in restraining cancer progression. Nat Med 2011;17:320–9. https://doi.org/10.1038/nm.2328.

[6] Öhlund D, Elyada E, Tuveson D. Fibroblast heterogeneity in the cancer wound. J Exp Med 2014;211:1503–23. https://doi.org/10.1084/jem.20140692.

[7] Orimo A, Gupta PB, Sgroi DC, Arenzana-Seisdedos F, Delaunay T, Naeem R, et al. Stromal fibroblasts present in invasive human breast carcinomas promote tumor growth and angiogenesis through elevated SDF-1/CXCL12 secretion. Cell 2005;121:335–48. https://doi.org/10.1016/j.cell.2005.02.034.

[8] Kalluri R, Zeisberg M. Fibroblasts in cancer. Nat Rev Cancer 2006;6:392–401. https://doi.org/10.1038/nrc1877.

[9] Cirri P, Chiarugi P. Cancer-associated-fibroblasts and tumour cells: A diabolic liaison driving cancer progression. Cancer Metastasis Rev 2012;31:195–208. https://doi.org/10.1007/s10555-011-9340-x.

[10] Zhang J, Liu J. Tumor stroma as targets for cancer therapy. Pharmacol Ther 2013;137:200–15. https://doi.org/10.1016/j.pharmthera.2012.10.003.

[11] Chen X, Song E. Turning foes to friends: targeting cancer-associated fibroblasts. Nat Rev Drug Discov 2019;18:99–115. https://doi.org/10.1038/s41573-018-0004-1.

[12] Span PN, Bussink J. Biology of hypoxia. Semin Nucl Med 2015;45:101–9. https://doi.org/10.1053/j.semnuclmed.2014.10.002.

[13] Brahimi-Horn MC, Chiche J, Pouysségur J. Hypoxia and cancer. J Mol Med 2007;85:1301–7. https://doi.org/10.1007/s00109-007-0281-3.

[14] Casazza A, Di Conza G, Wenes M, Finisguerra V, Deschoemaeker S, Mazzone M. Tumor stroma: A complexity dictated by the hypoxic tumor microenvironment. Oncogene 2014;33:1743–54. https://doi.org/10.1038/onc.2013.121.

[15] Gilkes DM, Semenza GL, Wirtz D. Hypoxia and the extracellular matrix: Drivers of tumour metastasis. Nat Rev Cancer 2014;14:430–9. https://doi.org/10.1038/nrc3726.

[16] Fitzmaurice C, Allen C, Barber RM, Barregard L, Bhutta ZA, Brenner H, et al. Global, regional, and national cancer incidence, mortality, years of life lost, years lived with disability, and disability-

adjusted life-years for 32 cancer groups, 1990 to 2015: A Systematic Analysis for the Global Burden of Disease Study Global Burden . JAMA Oncol 2017;3:524–48. https://doi.org/10.1001/jamaoncol.2016.5688.

[17] Ferlay J, Soerjomataram I, Ervik M, Dikshit R, Eser S, Mathers C, Rebelo M PD, Forman D, Bray F. GLOBOCAN 2012 v1.0, Cancer Incidence and Mortality Worldwide: IARC CancerBase. No. 11 [Internet]. Lyon, Fr Int Agency Res Cancer 2013;11:http://globocan.iarc.f.

[18] Tu K, Dou C, Zheng X, Li C, Yang W, Yao Y, et al. Fibulin-5 inhibits hepatocellular carcinoma cell migration and invasion by down-regulating matrix metalloproteinase-7 expression. BMC Cancer 2014;14:938. https://doi.org/10.1186/1471-2407-14-938.

[19] Fattovich G, Stroffolini T, Zagni I, Donato F. Hepatocellular carcinoma in cirrhosis: Incidence and risk factors. Gastroenterology, vol. 127, 2004. https://doi.org/10.1053/j.gastro.2004.09.014.

[20] Lin D, Wu J. Hypoxia inducible factor in hepatocellular carcinoma: A therapeutic target. World J Gastroenterol 2015;21:12171–8. https://doi.org/10.3748/wjg.v21.i42.12171.

[21] Zhang Q, Bai X, Chen W, Ma T, Hu Q, Liang C, et al. Wnt/β-catenin signaling enhances hypoxia-induced epithelial-mesenchymal transition in hepatocellular carcinoma via crosstalk with hif-1α signaling. Carcinogenesis 2013;34:962–73. https://doi.org/10.1093/carcin/bgt027.

[22] Wilson GK, Tennant DA, McKeating JA. Hypoxia inducible factors in liver disease and hepatocellular carcinoma: Current understanding and future directions. J Hepatol 2014;61:1397–406. https://doi.org/10.1016/j.jhep.2014.08.025.

[23] Anton D, Burckel H, Josset E, Noel G. Three-dimensional cell culture: A breakthrough in vivo. Int J Mol Sci 2015;16:5517–27. https://doi.org/10.3390/ijms16035517.

[24] Unger C, Kramer N, Walzl A, Scherzer M, Hengstschläger M, Dolznig H. Modeling human carcinomas: Physiologically relevant 3D models to improve anti-cancer drug development. Adv Drug Deliv Rev 2014;79:50–67. https://doi.org/10.1016/j.addr.2014.10.015.

[25] Ingram M, Techy GB, Saroufeem R, Yazan O, Narayan KS, Goodwin TJ, et al. Three-dimensional growth patterns of various human tumor cell lines in simulated microgravity of a NASA bioreactor. Vitr Cell Dev Biol - Anim 1997;33:459–66. https://doi.org/10.1007/s11626-997-0064-8.

[26] Ravi M, Paramesh V, Kaviya SR, Anuradha E, Paul Solomon FD. 3D cell culture systems: Advantages and applications. J Cell Physiol 2015;230:16–26. https://doi.org/10.1002/jcp.24683.

[27] Mehta G, Hsiao AY, Ingram M, Luker GD, Takayama S. Opportunities and Challenges for use of Tumor Spheroids as Models to Test Drug Delivery and Efficacy. J Control Release 2012;164:192–204. https://doi.org/10.1016/j.jconrel.2012.04.045.

[28] Cervantes-Gracia K, Husi H. Integrative analysis of Multiple Sclerosis using a systems biology approach. Sci Rep 2018;8:1–14. https://doi.org/10.1038/s41598-018-24032-8.

[29] Bindea G, Mlecnik B, Hackl H, Charoentong P, Tosolini M, Kirilovsky A, et al. ClueGO: A Cytoscape plug-in to decipher functionally grouped gene ontology and pathway annotation networks. Bioinformatics 2009;25:1091–3. https://doi.org/10.1093/bioinformatics/btp101.

[30] Luo YD, Fang L, Yu HQ, Zhang J, Lin XT, Liu XY, et al. p53 haploinsufficiency and increased mTOR

signalling define a subset of aggressive hepatocellular carcinoma. J Hepatol 2021;74:96–108. https://doi.org/10.1016/j.jhep.2020.07.036.

[31] Petrelli A, Perra A, Cora D, Sulas P, Menegon S, Manca C, et al. MicroRNA/gene profiling unveils early molecular changes and nuclear factor erythroid related factor 2 (NRF2) activation in a rat model recapitulating human hepatocellular carcinoma (HCC). Hepatology 2014;59:228–41. https://doi.org/10.1002/hep.26616.

[32] Zhang C, Peng L, Zhang Y, Liu Z, Li W, Chen S, et al. The identification of key genes and pathways in hepatocellular carcinoma by bioinformatics analysis of high-throughput data. Med Oncol 2017;34:101. https://doi.org/10.1007/s12032-017-0963-9.

[33] Ohnishi S, Murakami T, Moriyama T, Mitamura K, Imawari M. Androgen and estrogen receptors in hepatocellular carcinoma and in the surrounding noncancerous liver tissue. Hepatology 1986;6:440–3. https://doi.org/10.1002/hep.1840060320.

[34] Battello N, Zimmer AD, Goebel C, Dong X, Behrmann I, Haan C, et al. The role of HIF-1 in oncostatin M-dependent metabolic reprogramming of hepatic cells. Cancer Metab 2016;4:3. https://doi.org/10.1186/s40170-016-0141-0.

[35] Liang H, Block TM, Wang M, Nefsky B, Long R, Hafner J, et al. Interleukin-6 and oncostatin M are elevated in liver disease in conjunction with candidate hepatocellular carcinoma biomarker GP73. Cancer Biomarkers 2012;11:161–71. https://doi.org/10.3233/CBM-2012-00276.

[36] Martinez-Quetglas I, Pinyol R, Dauch D, Torrecilla S, Tovar V, Moeini A, et al. IGF2 Is Up-regulated by Epigenetic Mechanisms in Hepatocellular Carcinomas and Is an Actionable Oncogene Product in Experimental Models. Gastroenterology 2016;151:1192–205. https://doi.org/10.1053/j.gastro.2016.09.001.

[37] Kutmon M, van Iersel MP, Bohler A, Kelder T, Nunes N, Pico AR, et al. PathVisio 3: An Extendable Pathway Analysis Toolbox. PLoS Comput Biol 2015;11. https://doi.org/10.1371/journal.pcbi.1004085.

[38] Yang X, Zhang Y, Hosaka K, Andersson P, Wang J, Tholander F, et al. VEGF-B promotes cancer metastasis through a VEGF-A-independent mechanism and serves as a marker of poor prognosis for cancer patients. Proc Natl Acad Sci U S A 2015;112:E2900–9. https://doi.org/10.1073/pnas.1503500112.

[39] Sulas P, Di Tommaso L, Novello C, Rizzo F, Rinaldi A, Weisz A, et al. A Large Set of miRNAs Is Dysregulated from the Earliest Steps of Human Hepatocellular Carcinoma Development. Am J Pathol 2018;188:785–94. https://doi.org/10.1016/j.ajpath.2017.10.024.

[40] Guo W, Qiu Z, Wang Z, Wang Q, Tan N, Chen T, et al. MiR-199a-5p is negatively associated with malignancies and regulates glycolysis and lactate production by targeting hexokinase 2 in liver cancer. Hepatology 2015;62:1132–44. https://doi.org/10.1002/hep.27929.

[41] Eferl R, Wagner EF. AP-1: a double-edged sword in tumorigenesis. Nat Rev Cancer 2003;3:859–68. https://doi.org/10.1038/nrc1209.

[42] Behnke M, Reimers M, Fisher R. The expression of embryonic liver development genes in hepatitis c induced cirrhosis and hepatocellular carcinoma. Cancers (Basel) 2012;4:945–68. https://doi.org/10.3390/cancers4030945.

[43] Rudalska R, Dauch D, Longerich T, McJunkin K, Wuestefeld T, Kang TW, et al. In vivo RNAi screening identifies a mechanism of sorafenib resistance in liver cancer. Nat Med 2014;20:1138–46. https://doi.org/10.1038/nm.3679.

[44] Kimlin LC, Casagrande G, Virador VM. In vitro three-dimensional (3D) models in cancer research: An update. Mol Carcinog 2013;52:167–82. https://doi.org/10.1002/mc.21844.

[45] Luo D, Wang Z, Wu J, Jiang C, Wu J. The role of hypoxia inducible factor-1 in hepatocellular carcinoma. Biomed Res Int 2014;2014. https://doi.org/10.1155/2014/409272.

[46] Shen G, Li X. The Multifaceted Role of Hypoxia-Inducible Factor 1 (HIF1) in Lipid Metabolism. Hypoxia Hum. Dis., InTech; 2017. https://doi.org/10.5772/65340.

[47] Mahata B, Pramanik J, van der Weyden L, Polanski K, Kar G, Riedel A, et al. Tumors induce de novo steroid biosynthesis in T cells to evade immunity. Nat Commun 2020;11:1–15. https://doi.org/10.1038/s41467-020-17339-6.

[48] Hynes RO. Integrins: Bidirectional, allosteric signaling machines. Cell 2002;110:673–87. https://doi.org/10.1016/S0092-8674(02)00971-6.

[49] Park CC, Zhang H, Pallavicini M, Gray JW, Baehner F, Park CJ, et al. β1integrin inhibitory antibody induces apoptosis of breast cancer cells, inhibits growth, and distinguishes malignant from normal phenotype in three dimensional cultures and in vivo. Cancer Res 2006;66:1526–35. https://doi.org/10.1158/0008-5472.CAN-05-3071.

[50] White DE, Kurpios NA, Zuo D, Hassell JA, Blaess S, Mueller U, et al. Targeted disruption of β1-integrin in a transgenic mouse model of human breast cancer reveals an essential role in mammary tumor induction. Cancer Cell 2004;6:159–70. https://doi.org/10.1016/j.ccr.2004.06.025.

[51] Schaffner F, Ray AM, Dontenwill M. Integrin□??5??1, the fibronectin receptor, as a pertinent therapeutic target in solid tumors. Cancers (Basel) 2013;5:27–47. https://doi.org/10.3390/cancers5010027.

[52] Grzesiak JJ, Bouvet M. Determination of the ligand-binding specificities of the alpha2beta1 and alpha1beta1 integrins in a novel 3-dimensional in vitro model of pancreatic cancer. Pancreas 2007;34:220–8. https://doi.org/10.1097/01.mpa.0000250129.64650.f6.

[53] Kugler MC, Wei Y, Chapman H a. Urokinase receptor and integrin interactions. Curr Pharm Des 2003;9:1565–74. https://doi.org/10.2174/1381612033454658.

[54] Tyndall J, Kelso M, Clingan P, Ranson M. Peptides and Small Molecules Targeting the Plasminogen Activation System: Towards Prophylactic Anti-Metastasis Drugs for Breast Cancer. Recent Pat Anticancer Drug Discov 2008;3:1–13. https://doi.org/10.2174/157489208783478711.

[55] Shain KH, Yarde DN, Meads MB, Huang M, Jove R, Hazlehurst LA, et al. β1 integrin adhesion enhances IL-6-mediated STAT3 signaling in myeloma cells: Implications for microenvironment influence on tumor survival and proliferation. Cancer Res 2009;69:1009–15. https://doi.org/10.1158/0008-5472.CAN-08-2419.

[56] Kesanakurti D, Chetty C, Dinh DH, Gujrati M, Rao JS. Role of MMP-2 in the regulation of IL-6/Stat3 survival signaling via interaction with α5β1 integrin in glioma. Oncogene 2013;32:327–40. https://doi.org/10.1038/onc.2012.52.

[57] Lee KW, Yeo SY, Sung CO, Kim SH. Twist1 is a key regulator of cancer-associated fibroblasts. Cancer Res 2015;75:73–85. https://doi.org/10.1158/0008-5472.CAN-14-0350.

[58] Lin ZY, Chuang YH, Chuang WL. Cancer-associated fibroblasts up-regulate CCL2, CCL26, IL6 and LOXL2 genes related to promotion of cancer progression in hepatocellular carcinoma cells. Biomed Pharmacother 2012;66:525–9. https://doi.org/10.1016/j.biopha.2012.02.001.

[59] Enguita-Germán M, Fortes P. Targeting the insulin-like growth factor pathway in hepatocellular carcinoma. World J Hepatol 2014;6:716–37. https://doi.org/10.4254/wjh.v6.i10.716.

[60] Pan JH, Zhou H, Zhao XX, Ding H, Li W, Qin L, et al. Role of exosomes and exosomal microRNAs in hepatocellular carcinoma: Potential in diagnosis and antitumour treatments (Review). Int J Mol Med 2018;41:1809–16. https://doi.org/10.3892/ijmm.2018.3383.

[61] Kim HR, Roe JS, Lee JE, Cho EJ, Youn HD. P53 regulates glucose metabolism by miR-34a. Biochem Biophys Res Commun 2013;437:225–31. https://doi.org/10.1016/j.bbrc.2013.06.043.

[62] Lu L, Chen Y, Zhu Y. The molecular basis of targeting PFKFB3 as a therapeutic strategy against cancer. Oncotarget 2017;8:62793–802. https://doi.org/10.18632/oncotarget.19513.

[63] Shi W-K, Zhu X-D, Wang C-H, Zhang Y-Y, Cai H, Li X-L, et al. PFKFB3 blockade inhibits hepatocellular carcinoma growth by impairing DNA repair through AKT. Cell Death Dis 2018;9:428. https://doi.org/10.1038/s41419-018-0435-y.

[64] Li S, Dai W, Mo W, Li J, Feng J, Wu L, et al. By inhibiting PFKFB3, aspirin overcomes sorafenib resistance in hepatocellular carcinoma. Int J Cancer 2017;141:2571–84. https://doi.org/10.1002/ijc.31022.

[65] Taniguchi CM, Finger EC, Krieg AJ, Wu C, Diep AN, Lagory EL, et al. Cross-talk between hypoxia and insulin signaling through Phd3 regulates hepatic glucose and lipid metabolism and ameliorates diabetes. Nat Med 2013;19:1325–30. https://doi.org/10.1038/nm.3294.

[66] Yano H, Sakai M, Matsukawa T, Yagi T, Naganuma T, Mitsushima M, et al. PHD3 regulates glucose metabolism by suppressing stress-induced signalling and optimising gluconeogenesis and insulin signalling in hepatocytes. Sci Rep 2018;8:1–16. https://doi.org/10.1038/s41598-018-32575-z.

[67] Lu C, Fang S, Weng Q, Lv X, Meng M, Zhu J, et al. Integrated analysis reveals critical glycolytic regulators in hepatocellular carcinoma. Cell Commun Signal 2020;18. https://doi.org/10.1186/s12964-020-00539-4.

[68] Zhang Q, Qiao L, Liao J, Liu Q, Liu P, Liu L. A novel hypoxia gene signature indicates prognosis and immune microenvironments characters in patients with hepatocellular carcinoma. J Cell Mol Med 2021;25:3772–84. https://doi.org/10.1111/jcmm.16249.

[69] Dittmer J. The biology of the Ets1 proto-oncogene. Mol Cancer 2003;2. https://doi.org/10.1186/1476-4598-2-29.

[70] Ozaki I, Mizuta T, Zhao G, Yotsumoto H, Hara T, Kajihara S, et al. Involvement of the Ets-1 gene in overexpression of matrilysin in human hepatocellular carcinoma. Cancer Res 2000;60:6519–25.

[71] Ma N, Chen F, Shen SL, Chen W, Chen LZ, Su Q, et al. MicroRNA-129-5p inhibits hepatocellular carcinoma cell metastasis and invasion via targeting ETS1. Biochem Biophys Res Commun 2015;461:618–23. https://doi.org/10.1016/j.bbrc.2015.04.075.

[72] Placencio VR, DeClerck YA. Plasminogen activator inhibitor-1 in cancer: Rationale and insight for future therapeutic testing. Cancer Res 2015;75:2969–74. https://doi.org/10.1158/0008-5472.CAN-15-0876.

[73] Mitxelena J, Apraiz A, Vallejo-rodr J, Garc I, Fullaondo A, Malumbres M, et al. An E2F7-dependent transcriptional program modulates DNA damage repair and genomic stability. Nucleic Acids Res 2018:1–14. https://doi.org/10.1093/nar/gky218.

[74] Yim KHW, Hrout A Al, Borgoni S, Chahwan R. Extracellular vesicles orchestrate immune and tumor interaction networks. Cancers (Basel) 2020;12:1–23. https://doi.org/10.3390/cancers12123696.

[75] Cui L, Hu Y, Bai B, Zhang S. Serum miR-335 Level is Associated with the Treatment Response to Trans-Arterial Chemoembolization and Prognosis in Patients with Hepatocellular Carcinoma. Cell Physiol Biochem 2015;37:276–83. https://doi.org/10.1159/000430352.

[76] Wang F, Li L, Piontek K, Sakaguchi M, Selaru FM. Exosome miR-335 as a novel therapeutic strategy in hepatocellular carcinoma. Hepatology 2018;67:940–54. https://doi.org/10.1002/hep.29586.

[77] Wu J, Zhu AX. Targeting insulin-like growth factor axis in hepatocellular carcinoma. J Hematol Oncol 2011;4. https://doi.org/10.1186/1756-8722-4-30.

[78] Akazawa Y, Kono H, Hara M, Furuya S, Nakata Y, Wakana H, et al. M-CSF receptor antagonists inhibit the initiation and progression of hepatocellular carcinoma in mice. Anticancer Res 2019;39:4787–94. https://doi.org/10.21873/anticanres.13663.

[79] Landskron G, De La Fuente M, Thuwajit P, Thuwajit C, Hermoso MA. Chronic inflammation and cytokines in the tumor microenvironment. J Immunol Res 2014;2014. https://doi.org/10.1155/2014/149185.

[80] Zhang Z, Lei B, Chai W, Liu R, Li T. Increased expression of insulin-like growth factor-1 receptor predicts poor prognosis in patients with hepatocellular carcinoma. Medicine (Baltimore) 2019;98:e17680. https://doi.org/10.1097/MD.0000000000017680.

[81] Jiang L, Liu QL, Liang QL, Zhang HJ, Ou WT, Yuan G Le. Association of PHD3 and HIF2α gene expression with clinicopathological characteristics in human hepatocellular carcinoma. Oncol Lett 2018;15:545–51. https://doi.org/10.3892/ol.2017.7302.

FIGURE LEGENDS

Figure 1. Experimental model and initial validations. a) Schematic depiction of experimental groups. b) Bright field images of 2D/ 3D HepG2 and fibroblasts cultures fixed and stained with crystal violet and 3D fibroblasts fixed and stained with neutral red (scale bar = 50 µm). c) Cell viability of HepG2 cells after treatment with increasing concentrations of $CoCl_2$ for 6 hours ($p < 0.01$). d) HIF1-α protein expression was detected in $CoCl_2$ HepG2-treated cells after 6 hours of incubation. Uncropped blots are shown in Fig. S1. e) Immunofluorescence detection of HIF1-α expression and localization in HepG2 cells incubated with or without $CoCl_2$ (scale bar = 20 µm).

Figure 2. **Computational analysis of the RNA-Seq of our group cohorts.** a) Hierarchical clustering heatmap of global expression in all groups (in triplicates) was generated with Morpheus using default settings. B) PCA plot based on global expression in all groups (in triplicates) was generated using NetworkAnalyst c) PCA plot based on significant DEGs of group 2,3,4,5 in comparison to group 1. d) Venn diagrams showing the common and unique upregulated genes and downregulated genes of groups 2, 3, 4, and 5. The interactive diagrams can be accessed online using the InteractiVenn (http://www.interactivenn.net) and uploading supplementary files 1 & 2c)

Figure 3. Pathway clustering analysis and heatmap representation of experimental groups. a) Pathway term clustering based on KEGG pathway maps based on DEGs of experimental groups. All groups are compared to G1 as the control condition. Node size of pathway terms resemble the number of associated genes to it. The stronger the node color the more significant a cluster is. b) ORA heatmaps of enriched genes in denoted pathways based on KEGG from all groups. Heatmaps were generated using NetworkAnalyst.

Figure 4. Customized Insulin signaling pathway map of Group 5 DEGs. Insulin signaling pathway identified as significant through ClueGO/CluePedia pathway term clustering analyzed and customized through Pathvisio. Red boxes: up regulated genes; green boxes: down regulated genes; gray boxes: genes not found within the DEGs. Color intensity resembles the deregulated status of the gene from the LogFC scale (between a 1 to -1 LogFC). A clear up-regulated trend was identified that resembles the activation of the pathway and the main genes involved within this mechanism. This customized pathway map delineates the line of significance from G5 Insulin signaling pathway. These results back-up and

validate ClueGO/CluePedia analysis. Yellow and blue stars highlight the genes/proteins that were further validated either through antibody arrays or qPCR respectively.

Figure 5. Confirmation studies using genomic, proteomic, and clinical analyses. a) Validation by qPCR. RNA-Seq based expression was plotted against qPCR-based expression. qPCR data are represented as means of fold change ± SD. b-f) levels of different secreted factors in 3D mono- and co-cultures analyzed by antibody arrays. Experimental scheme is outlined in Fig. S2 g) fold change of expression of HepG2 and Fibroblasts before and after co-culture for markers shown in panels b-f based on RNA-seq data. h) western blotting of total cell lysates of 2D or 3D HepG2 cultures. Uncropped blots are shown in Fig. S3. i-j) Kaplan–Meier curves of progression-free survival of IGF1R and EGLN3 in HCC patients.

SUPPLEMENTARY INFORMATION

Supplementary data: materials and methods, and supplementary figures

Table S1: Canonical pathways list

Table S2: miRNA gene interaction list

Supplementary document1: Venn Dr file

Supplementary document2: Venn Ur file

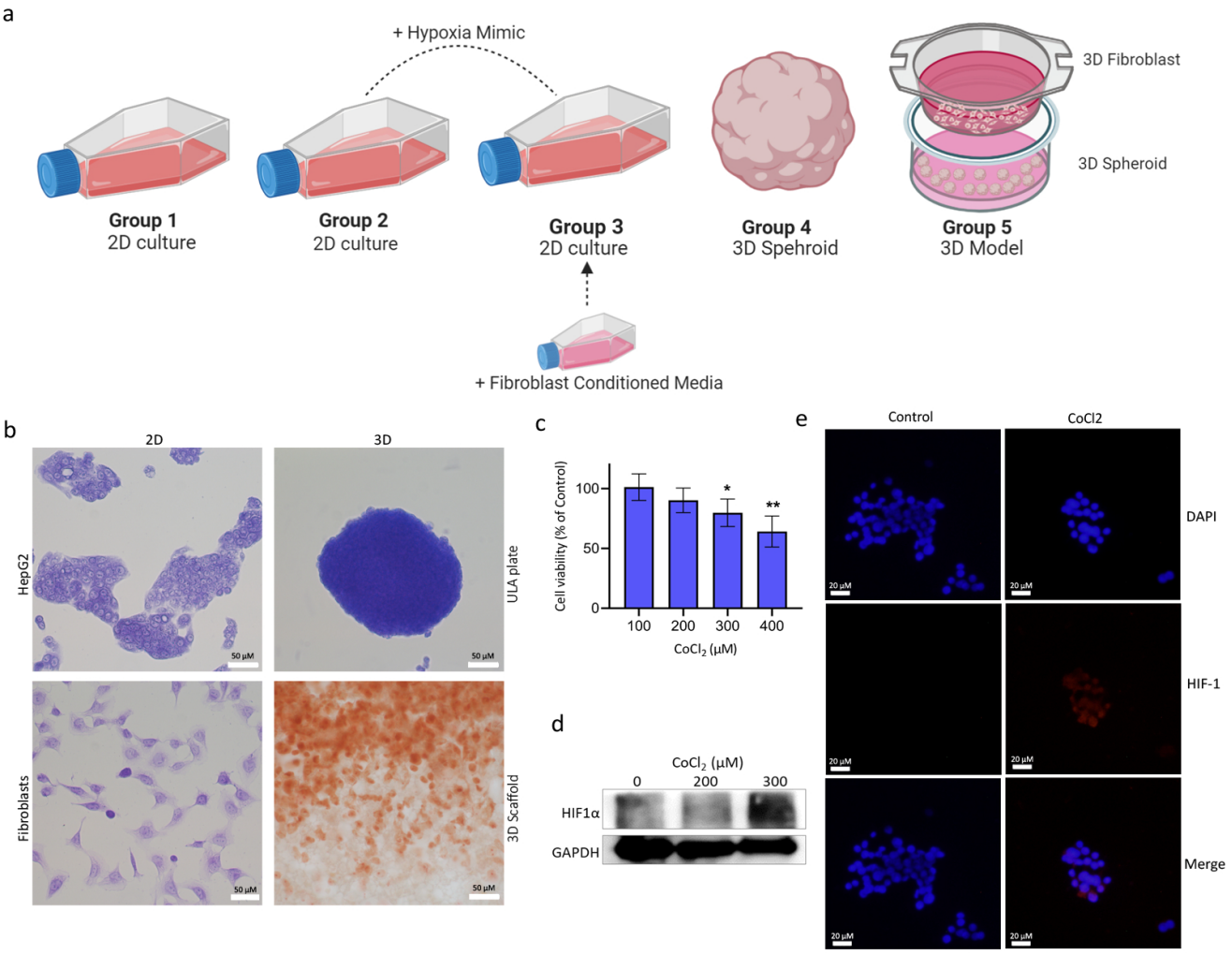

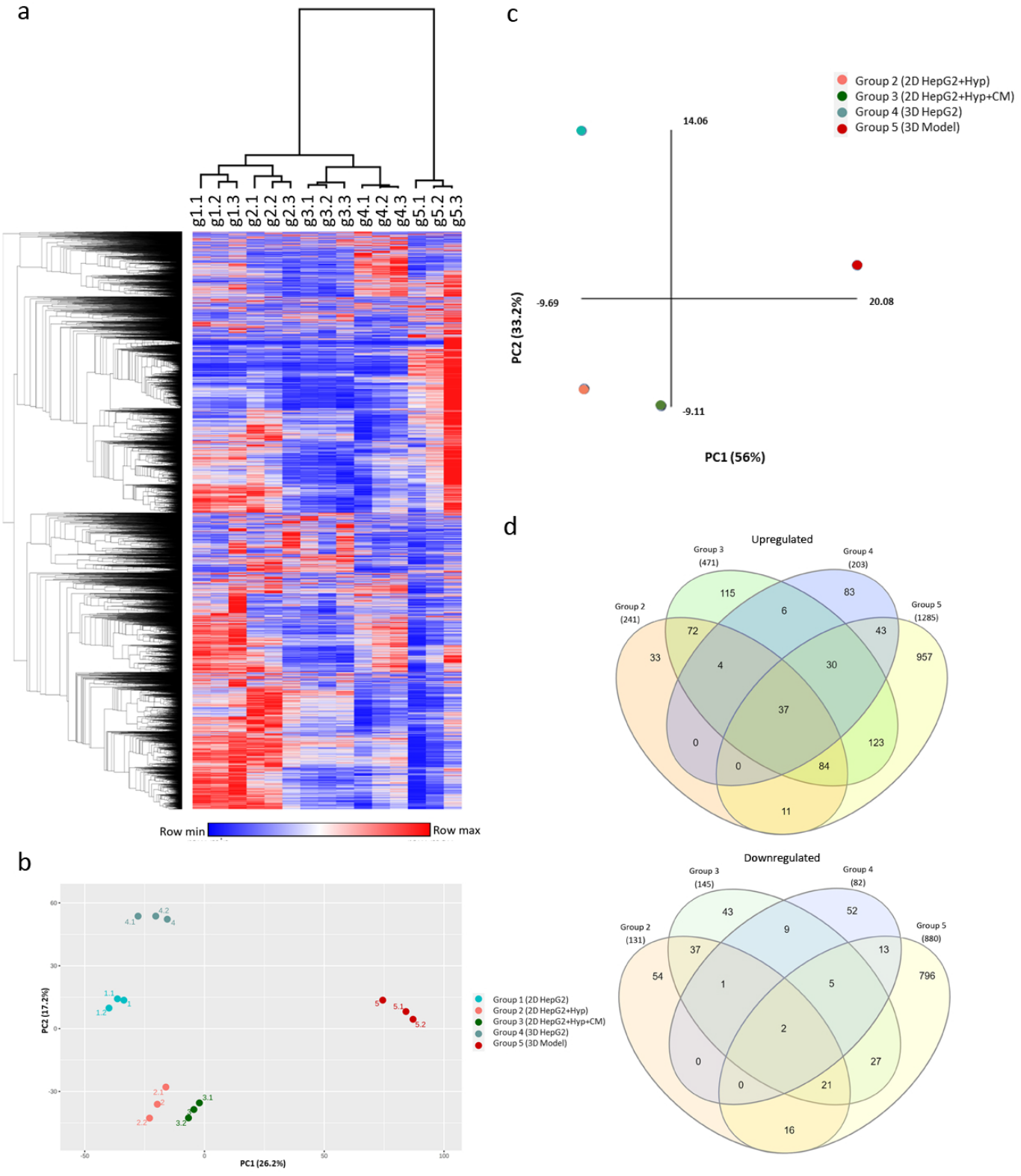

a

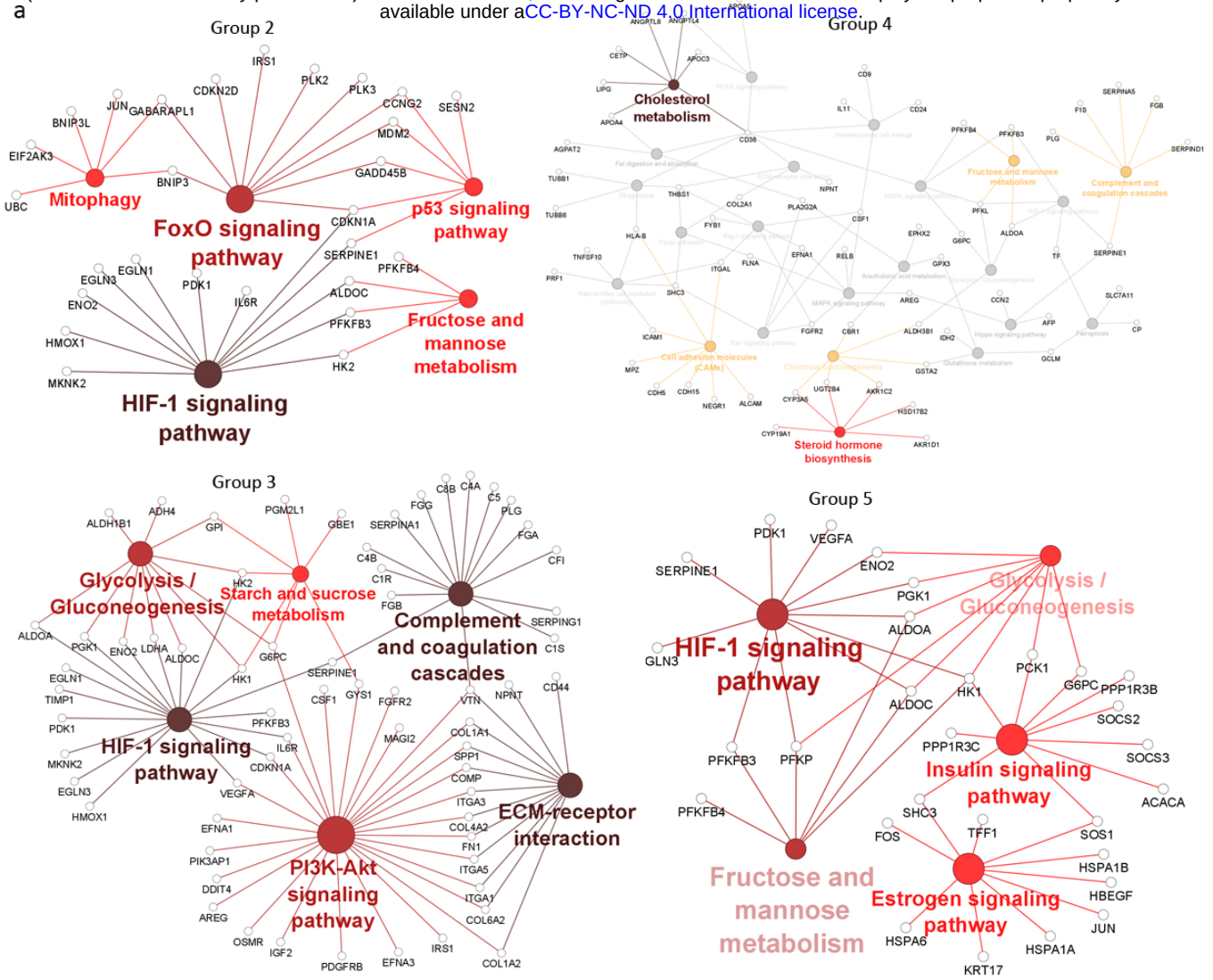

b